[^{125}I]Iberiotoxin-D19Y/Y36F, the First Selective, High Specific Activity Radioligand for High-Conductance Calcium-Activated Potassium Channels

Alexandra Koschak,[‡] Robert O. Koch,[‡] Jessica Liu,[§] Gregory J. Kaczorowski,[§] Peter H. Reinhart,[||] Maria L. Garcia,[§] and Hans-Günther Knaus*,[‡]

Institut für Biochemische Pharmakologie, Peter Mayr-Strasse 1, A-6020 Innsbruck, Austria, Department of Membrane Biochemistry and Biophysics, Merck Research Laboratories, P.O. Box 2000, Rahway, New Jersey 07065, and Department of Neurobiology, Duke University Medical Center, P.O. Box 3209, Durham, North Carolina 27710

Received August 16, 1996; Revised Manuscript Received October 29, 1996[⊗]

ABSTRACT: Iberiotoxin (IbTX), a selective peptidyl ligand for high-conductance Ca^{2+}-activated K^+ (maxi-K) channels cannot be radioiodinated in biologically active form due to the importance of Y36 in interacting with the channel pore. Therefore, an IbTX double mutant (IbTX-D19Y/Y36F) was engineered, expressed in *Escherichia coli*, purified to homogeneity, and radiolabeled to high specific activity with ^{125}I. IbTX-D19Y/Y36F and [^{127}I]IbTX-D19Y/Y36F block maxi-K channels expressed in *Xenopus laevis* oocytes with equal potency as wild-type IbTX ($K_d \sim 1$ nM). Under low ionic strength conditions, [^{125}I]IbTX-D19Y/Y36F binds with high affinity to smooth muscle sarcolemmal maxi-K channels (K_d of 5 pM, as determined by either equilibrium binding or kinetic binding analysis), and with a binding site density of 0.45 pmol/mg of protein. Competition studies with wild-type IbTX, IbTX-D19Y/Y36F or charybdotoxin (ChTX) result in complete inhibition of binding whereas toxins selective for voltage-gated K^+ channels (margatoxin (MgTX) or α-dendrotoxin (α-DaTX)) do not have any effect on IbTX binding. Indole diterpene alkaloids, which are selective inhibitors of maxi-K channels, and potassium ions both modulate [^{125}I]IbTX-D19Y/Y36F binding in a complex manner. This pattern is also reflected during covalent incorporation of the radiolabeled toxin into the 31 kDa β-subunit of the maxi-K channel in the presence of a bifunctional cross-linking reagent. In rat brain membranes, IbTX-D19Y/Y36F does not displace binding of [^{125}I]MgTX or [^{125}I]-α-DaTX to sites associated with voltage-gated K^+ channels, nor do these latter toxins inhibit [^{125}I]IbTX-D19Y/Y36F binding. Taken together, these results demonstrate that [^{125}I]IbTX-D19Y/Y36F is the first selective radioligand for maxi-K channels with high specific activity.

High-conductance Ca^{2+}-activated K^+ (maxi-K)[1] channels comprise a group of ion channels that are expressed in skeletal and smooth muscle, neurons, kidney, adrenal chromafin cells, insulin-producing cells, and pituitary cells, as well as fibroblasts (Miller et al., 1985; Reinhart et al., 1989; Vázquez et al., 1989; Knaus et al., 1996; Zweifach et al., 1991; Solaro & Lingle, 1992; Oosawa et al., 1992; Rane, 1991; Wang et al., 1994; Kaczorowski et al., 1996). Gating of these channels is modulated by elevation of intracellular Ca^{2+} and membrane depolarization, and they display a large single-channel conductance (200−300 pS), as well as high selectivity for K^+ (Latorre et al., 1989). Maxi-K channels are sensitive to extracellular application of several peptidyl toxins [e.g., charybdotoxin (ChTX) or iberiotoxin (IbTX)] which bind with high affinity to a receptor site located in the external vestibule of the channel, thereby preventing K^+ flux by physically occluding the pore (Anderson et al., 1988; MacKinnon & Miller, 1988; Park et al., 1991; Stampe et al., 1994). In addition, a number of non-peptidyl modulators of these channels have recently been identified. These include glycosylated triterpenes (e.g., the soyasaponins), which bind to a site accessible from the inside of the channel to increase channel activity (McManus et al., 1993), and indole diterpenes (e.g., paxilline and aflatrem), which are the most potent non-peptidyl maxi-K channel inhibitors identified to date (Knaus et al., 1994c). Employing [^{125}I]ChTX, it has been possible to define the pharmacology and to purify maxi-K channels from aortic and tracheal smooth muscle (Kaczorowski et al., 1996; Giangiacomo et al., 1995; Garcia-Calvo et al., 1994). In these tissues, the purified maxi-K channel consists of two subunits (α and β) that are sufficient to form fully functional maxi-K channels when reconstituted into planar lipid bilayers (Giangiacomo et al., 1995; Garcia-Calvo et al., 1994; Knaus et al., 1994b). Amino acid sequence obtained from proteolytic fragments of the α- and β-subunits, as well as by low-stringency hybridization protocols enabled the cloning of the maxi-K channel α- and β-subunits (Butler et al., 1993; Knaus et al., 1994a,b; Tseng-Crank et al., 1994).

[†] H.-G.K. was supported by Grants S6611-MED and P11187-MED from the Austrian Research Foundation and by Grant #6239 from the Austrian National Bank. H.-G.K. is a recipient of an APART fellowship award provided by the Austrian Academy of Sciences. P.H.R. was supported in part by NIH Grant NS31253.

* Correspondence should be addressed to H.-G.K. Tel: +43-512-507-3156. FAX: +43-512-507-2858. E-mail: hans.g.knaus@uibk.ac.at. R.O.K. contributed equally to this work.

[‡] IBP.

[§] Merck Research Laboratories.

[||] Duke University Medical Center.

[⊗] Abstract published in *Advance ACS Abstracts,* January 15, 1997.

[1] Abbreviations: BSA, bovine serum albumin; ChTX, charybdotoxin; DaTX, dendrotoxin; DSS, disuccinimidyl suberate; K_{+1}, association rate constant; k_{-1}, dissociation rate constant; K_d, dissociation constant; K_i, inhibition constant; IbTX, iberiotoxin; MgTX, margatoxin; maxi-K channel, high-conductance calcium-activated potassium channel; NxTX, noxiustoxin; SDS−PAGE, sodium dodecyl sulfate−polyacrylamide gel electrophoresis; TEA, tetraethylammonium.

S0006-2960(96)02074-0 CCC: $14.00

In addition to its interaction with maxi-K channels, ChTX also inhibits representatives of the *Shaker* family of voltage-gated K^+ channels (e.g., $K_v1.2$ and $K_v1.3$) which are expressed in neurons, T-lymphocytes, and osteoclasts (Vázquez et al., 1990; Deutsch et al., 1991; Arkett et al., 1994), and [^{125}I]ChTX binds with high affinity to these channels in brain and T-lymphocytes (Vázquez et al., 1990; Deutsch et al., 1991). Moreover, high-affinity interaction of ChTX has also been reported for low- and intermediate-conductance Ca^{2+}-activated K^+ channels in smooth muscle cell lines, *Aplysia* neurons, human T-lymphocytes, and erythrocytes (Hermann & Erxleben, 1987; Van Renterghem & Lazdunski, 1992; Leonard et al., 1992; Brugnara et al., 1993a,b).

Due to the promiscuity of [^{125}I]ChTX, the investigation of maxi-K channels by radioligand binding was hampered in most tissues except smooth muscle. Because of that, limited information is available for other maxi-K channels, such as those expressed in skeletal muscle, renal or neuronal tissue. Recently a biologically active radiolabeled derivative of IbTX was prepared by substituting Asp19 for Cys and subsequently coupling this toxin analog to [^{3}H]-*N*-ethylmaleimide (Knaus et al., 1996). [^{3}H]NEM-IbTX-D19C has been useful in identifying maxi-K channels in rat brain membranes, a tissue in which the use of [^{125}I]ChTX was hampered by the presence of relatively high densities of ChTX-sensitive voltage-gated K^+ channels ($K_v1.2$ and $K_v1.3$) (Wang et al., 1994). In this manuscript, we report the expression, purification and pharmacological characterization of [^{125}I]IbTX-D19Y/Y36F, the first selective, high specific activity radioligand for maxi-K channels. This radioligand should now facilitate a detailed analysis of the molecular pharmacology of maxi-K channels in all tissues with low channel densities.

EXPERIMENTAL PROCEDURES

Materials. Escherichia coli DH5α was used for plasmid propagation and strain BL21(DE3) was used for expression of the fusion protein. Plasmid PGEMEX-1 was from Promega. Prestained molecular weight standards (range 14.4−106 kDa) were obtained from Bio-Rad. Endoproteinase Lys-C was from Boehringer Mannheim. Synthetic ChTX was purchased from Peninsula Laboratories. Na[^{125}I] was bought from New England Nuclear Corp. Glass fiber filters (GF/C) were from Whatman. Polyethyleneimine and bovine serum albumin were purchased from Sigma. All other reagents were obtained from commercial sources and were of the highest purity grade commercially available.

Plasmid Construction, Synthesis, and Purification of Recombinant IbTX-D19Y/Y36F. The plasmid pG9IbTX-D19Y/Y36F, encoding six histidine residues between the fusion protein and the factor Xa cleavage site and the wild-type IbTX sequence was constructed as described in Knaus et al. (1996). This plasmid was altered such that codon 19 of IbTX was transformed from Asp to Tyr and codon 36 from Tyr to Phe and sequenced (Sanger et al., 1977). The fusion protein was expressed in *E. coli* and purified essentially as described (Garcia-Calvo et al., 1993). Fractions containing the fusion protein were identified by Coomassie staining of SDS−PAGE gels, combined, and dialyzed overnight against 20 mM Tris/HCl, 50 mM NaCl, 0.5 mM β-mercaptoethanol, pH 8.0. After dialysis, the fusion protein was concentrated (Centriprep-10, Amicon Inc.) and incubated with trypsin for 30 min at room temperature, at a substrate: enzyme ratio of 50:1, and the resulting fragments separated by chromatography on a Mono-S HR5/5 cation-exchange column (Pharmacia) equilibrated with 20 mM sodium borate, pH 9.0. Elution of bound material was achieved in the presence of a linear gradient of NaCl (0−750 mM NaCl over 60 min) at a flow rate of 0.5 mL/min. The fraction which contains IbTX-D19Y/Y36F was identified in radioligand binding studies (Vázquez et al., 1989) and subsequently incubated with 5% acetic acid at 45 °C for 72 h to achieve complete cyclization of the amino-terminal glutamic acid residue. The sample was then applied to a C_{18} reversed-phase HPLC column (Vydac, 1.0 × 25 cm) and elution was carried out using conditions identical to those previously reported for wild-type IbTX (Galvez et al., 1990). Composition of the purified material was verified by electrospray mass spectroscopy. Aliquots were lyophilized and stored at −80 °C.

Amino Acid Sequence Analysis of IbTX-D19Y/Y36F. Purified, uncyclized IbTX-D19Y/Y36F was reduced, subjected to alkylation with iodoacetic acid (Gimenez-Gallego et al., 1988), and re-purified by reversed-phase chromatography as described above. Approximately 200 pmol of reduced and alkylated IbTX-D19Y/Y36F was loaded onto a Porton peptide filter support, and automated Edman degradation was performed using a Porton 2090 microsequencer. Phenylthiohydantoin amino acid derivatives were analyzed using an on-line detection system with typical repetitive yields of ∼97%. The corresponding arginine residues in IbTX-D19Y/Y36F at positions 25 and 34 have not been detected by amino-terminal sequencing because of the low binding to the filter support. Therefore, IbTX-D19Y/Y36F was digested with endoproteinase Lys-C (molar ratio of enzyme to IbTX-D19Y/Y36F 1:10), and the yielded fragments were purified by reversed-phase chromatography and sequenced (Gimenez-Gallego et al., 1988).

Iodination of IbTX-D19Y/Y36F. 10 μg (2.4 nmol) of IbTX-D19Y/Y36F dissolved in 50 μL of 200 mM sodium phosphate, pH 7.3, were incubated for 15 min at room temperature with 2−3 mCi [^{125}I]Na (20−30 μL) in the presence of 1% β-D-glucose (25 μL) and Enzymobeads (50 μL; Bio-Rad). The reaction mixture was briefly spun at 1000*g*, applied to a C_{18} reversed-phase column (Vydac; 0.45 × 25 cm), and eluted with a linear gradient from 17% to 28% acetonitrile in 0.05% TFA. The radioiodinated peptide was lyophilized in the presence of 0.1% BSA and resuspended in 150 mM NaCl, 20 mM Tris/HCl, pH 7.4, and stored at −80 °C. Identical conditions have been used for iodinations employing [^{127}I]Na. Material judged to be a mono-iodo derivative based on specific activity of the iodinated peptide was subjected to amino acid sequence determination by automated Edman degradation to confirm iodination in the residue at position 19. Increasing the ratio of NaI to peptide did not improve the yields of mono-iodotyrosine-IbTX-D19Y/Y36F but led to the appearance of other iodinated species upon reversed-phase chromatography (data not shown).

Electrophysiological Recordings. The hbr1 variant of the high-conductance Ca^{2+}-activated K^+ channels cloned from a human brain cDNA library (Tseng-Crank et al., 1994) was expressed in *Xenopus* oocytes as follows: plasmid DNA in pBluescript was purified using Qiagen (Chatsworth, CA) mini-prep columns, linearized using restriction endonucleases

(New England Biolabs, Beverly, MA), and transcribed using the Ambion MEGAscript kit (Austin, TX) in the presence of the cap analog m7G(5i)ppp(5i)G (Ambion). RNA was resuspended in an RNase-free buffer (50 mM KCl, 5 mM HEPES pH 7.0), and examined on ethidium bromide-stained denaturing agarose mini-gels to assure the presence of a single undegraded band of the expected size.

Female *Xenopus laevis* were obtained from Nasco (Fort Atkinson, WI). Stage V−VI oocytes (Dumont, 1972) were kept in Frog-92 medium (92 mM NaCl, 1.5 mM KCl, 1.2 mM $CaCl_2$, 2 mM $MgCl_2$, 10 mM HEPES, 50 μg/mL gentamycin, pH 7.6) and kept at 17 °C for 24 h prior to RNA injection. Each oocyte was injected with 40 nL of cRNA (diluted to 100 ng/mL) using a Drummond Nanojector (Broomall, PA). Oocytes were maintained at 17 °C in Frog-92 medium which was changed daily. The expression of maxi-K currents in oocytes was assayed by a two-electrode voltage clamp. Electrodes were prepared from WPI TW-100F-3 glass (World Precision Instruments) and filled with 3 M KCl. Electrode resistances were 1.5−2.2 MΩ. Currents were amplified using an Axoclamp 2B amplifier (Axon Instruments, Foster City, CA), low-pass filtered at 2 kHz using an eight-pole Bessel filter (Frequency Devices, Haverhill, MA), and digitized by an Axon AD/DA converter (TL-1 DMA interface). Ohmic leak currents and capacitance currents were subtracted using a P/4 protocol. Grounding was achieved via an agar bridge to avoid junction potential shifts caused by solution changes.

Recording solutions used gluconate as a non-permeant anion to reduce the activation of Ca^{2+}-activated chloride channels endogenous to oocytes (Miledi, 1982). The bath solution consisted of 90 mM sodium gluconate, 2.5 mM K^+gluconate, 5 mM $CaCl_2$, 1 mM $MgCl_2$, and 10 mM HEPES, pH 7.4. Oocytes were clamped at −80 mV and currents were elicited by 100 ms voltage steps from 0 mV to +100 mV in 10 mV increments. Bath solutions were exchanged using computer-controlled solenoid valves controlling a gravity-flow perfusion system (2 mL/min). The oocyte was positioned in a laminar flow chamber (volume approximately 500 μL) to ensure rapid solution exchange. IbTX stock solutions were diluted into the perfusion buffer immediately prior to use. For IbTX concentrations 10 nM and higher, IbTX was applied for 10 min, while for concentrations below 10 nM, the toxins were applied for 20 min to ensure equilibrium binding had been achieved. At these times, currents were recorded and plotted as fractions of the maximal currents observed prior to drug addition. All solutions were equilibrated at room temperature (22−25 °C) before use. Salts of the highest available purity were obtained from Fluka Chemica.

Binding Assays and Preparation of Bovine Tracheal Smooth Muscle Sarcolemmal Membrane Vesicles. All binding assays were carried out in 12 × 75 mm polystyrene tubes (Sarstedt No. 55.467). The incubation medium (0.5−1 mL) consisted of 20 mM Tris/HCl, pH 7.4, 10 mM NaCl, and 0.1% BSA (buffer A). Nonspecific binding was defined in the presence of 10 nM synthetic ChTX or recombinant IbTX, and incubation was carried out at 22−25 °C typically for >15 h. Experiments with low receptor and/or radioligand concentrations (e.g., saturation studies) were allowed to reach equilibrium for 60−72 h without any detectable decay in receptor activity. All serial toxin dilutions were performed in a BSA-containing buffer and directly added to the incubation mixture to avoid adsorption phenomena. Drug dilutions were made similarly from a DMSO stock solution. A final DMSO concentration of 0.5% was never exceeded, and this concentration was without effect on binding (data not shown). At the end of incubation, the reaction mixture was rapidly filtered through Whatman GF/C glass fiber filters that had been presoaked for at least 60 min in 0.3% (w/v) polyethyleneimine, followed by two washes with ice-cold filtration buffer (20 mM Tris/HCl, pH 7.4, 150 mM NaCl; 4 mL per wash). A Brandell cell harvester was used to perform the filtration procedure. Employing this protocol, and at a K_d concentration of radioligand and receptor, nonspecific binding represented less than 3% of the total amount of radioactivity added, and specific binding is >95% of total binding. No displaceable binding of [^{125}I]IbTX-D19Y/Y36F was detected from GF/C filters under these conditions. In each experiment, duplicate or triplicate assays were routinely performed, and the data were averaged. Preparation of bovine tracheal smooth muscle sarcolemmal membrane vesicles was performed as described previously (Slaughter et al., 1989).

Cross-Linking Experiments. Bovine tracheal smooth muscle sarcolemmal membrane vesicles (0.1 mg/mL) were incubated with 20−40 pM [^{125}I]IbTX-D19Y/Y36F in 20 mM Tris/HCl, pH 7.4, 10 mM NaCl, 0.1% BSA until equilibrium was achieved (>15 h at room temperature). The membranes were washed twice with ice-cold 100 mM Na−PO_4^{3-} buffer, pH 8.5. Disuccinimidyl suberate dissolved in DMSO (100 mM) was added with vigorous agitation up to a final concentration of 0.2 mM, and allowed to react for 2 min on ice. Thereafter, the incubation mixture was adjusted to a final concentration of 100 mM Tris/HCl, pH 7.4, to quench the unreacted cross-linking reagent. The membranes were collected by centrifugation (45000*g* for 15 min), washed twice in buffer as above, resuspended in SDS−PAGE sample buffer (4−6% SDS, 1% β-mercaptoethanol) and separated by 12% SDS−PAGE. The gels were dried and subjected to autoradiography at −80 °C for 3−7 days using Kodak XAR film.

Analysis of Data: Radioligand Binding Studies. The results from saturation binding experiments were subjected to a Scatchard analysis, and linear regression was performed to obtain the equilibrium dissociation constant (K_d) and maximal receptor concentration (B_{max}). The correlation coefficient for these plots was typically >0.98. Data from competition experiments were computer-fitted to the general dose−response equation (DeLean et al., 1978), and then analyzed by a previously published method (Linden, 1982) to determine K_i values. The association rate constant (k_{+1}) was determined by employing both the pseudo-first-order rate equation [$k_{+1} = k_{obs}(RL_{equib}/(R_0L_0)$] and the second-order rate equation $k_{+1} = [1/(L_0-R_0)][(L_0 - RL_t)/(R_0 - RL_t)]$, where L_0 is the total concentration of ligand, R_0 the total receptor concentration, RL is the receptor−ligand complex at one given time point, *t*, and RL_{equib} is the receptor−ligand complex at equilibrium. The dissociation rate constant (k_{-1}) for [^{125}I]IbTX-D19Y/Y36F was determined from the first-order plot of ligand dissociation versus time.

Protein Determination. The concentration of membrane protein was determined by a previously published method using BSA as a standard (Bradford, 1976).

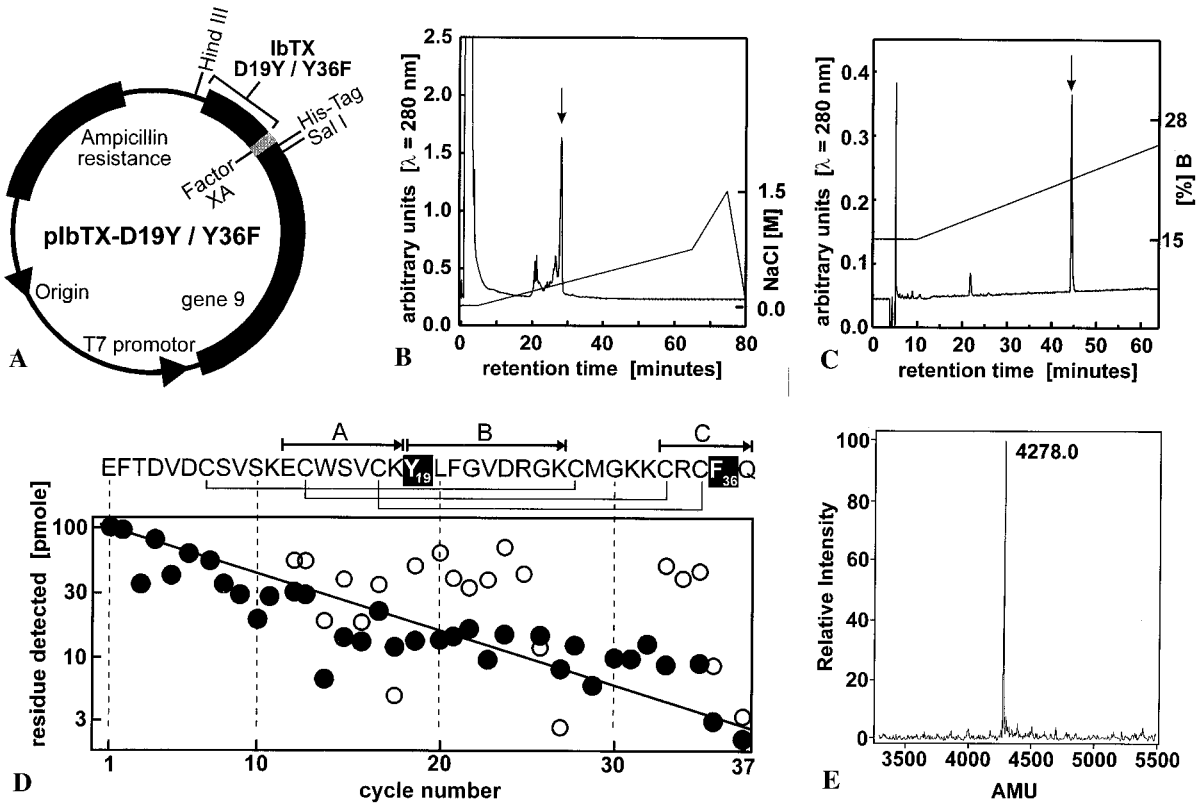

FIGURE 1: Design of the synthetic IbTX-D19Y/Y36F gene, its purification, sequence confirmation, and electrospray mass spectroscopy. (A) The plasmid map of pIbTX-D19Y/Y36F shows the location of the synthetic IbTX-D19Y/Y36F gene, the Factor XA cleavage site, and the T7 gene 9 fusion protein. (B) Cation-exchange chromatography. ~100 mg of trypsin-digested fusion protein was loaded onto a Mono-S HR5/5 column equilibrated in 20 mM sodium borate, pH 9.0, and the gradient was applied at a rate of 0.75 M NaCl/h. The arrow indicates elution of IbTX-D19Y/Y36F. (C) Reversed-phase chromatography. The active fraction of the Mono-S run was applied to a C_{18} reversed-phase column as described under Experimental Procedures. The arrow indicates elution of IbTX-D19Y/Y36F. (D) Upper panel, amino acid sequence determination of IbTX-D19Y/Y36F. IbTX-D19Y/Y36F was HPLC-purified without prior cyclization of the amino-terminal residue, reacted with iodoacetic acid, and the alkylated toxin purified by reversed-phase HPLC. The substituted residues in position 19 and 36 are high-lighted. The arrows A, B, and C indicate sequence of internal IbTX-D19Y/Y36F fragments after digesting the toxin with endoproteinase Lys-C and isolation of the respective fragments by reversed-phase HPLC. Amino-terminal Edman degradation was carried out on a Porton microsequencer using standard techniques. Lower panel, the logarithm of the amount of detected phenylthiohydantoin derivatives from each cycle of amino-terminally sequenced IbTX-D19Y/Y36F (●) or internal toxin fragments (○) is plotted versus the cycle number. (E) Electrospray mass spectroscopy of IbTX-D19Y/Y36F. Peptides were analyzed on a Finigan-MAT 700 in the electrospray ionization mode. The raw data were deconvoluted by the Finigan BIOMASS program to allow the assignment of a unique molecular weight. Uncyclized IbTX-D19Y/Y36F was found by electrospray mass spectroscopy to have a molecular weight of 4278.0 Da, a number which is in excellent agreement with the calculated molecular weight of 4277.85 Da.

RESULTS

Expression, Purification, and Sequence Analysis of IbTX-D19Y/Y36F. IbTX is the most selective peptidyl probe for maxi-K channels described to date, but its radioiodination in biologically active form has not been achieved so far; all attempts to iodinate Tyr36 have resulted in biologically inactive material. In an effort to overcome this problem, we constructed a synthetic IbTX gene and altered two residues in such a way that IbTX-Asp19 was mutated to a Tyr residue, and IbTX-Tyr36 was replaced by Phe (Figure 1A). The rationale for modifying these positions relies on well-known structural information concerning the interaction surface of ChTX with maxi-K channels. Since the three-dimensional NMR structure of IbTX and ChTX are very similar, it was postulated that position 19 could be modified without loss of activity, whereas only conservative substitutions at position 36 would be allowed.

In order to characterize such an IbTX variant in detail, the protein was expressed in *E. coli* as part of a fusion protein with the T7 gene 9 product. After isolating the fusion protein, forming the toxin's disulfide bridges and cleavage of the fusion protein with trypsin to release IbTX-D19Y/Y36F, the peptide was purified by cation exchange (Figure 1B) and reversed-phase chromatography (Figure 1C). Since cyclization of the amino-terminal glutamic acid residue was previously shown to be absolutely required for high-affinity interaction with maxi-K channels (Galvez et al., 1990) the partially purified preparation was exposed to 5% acetic acid at 45 °C for 72 h prior to reversed-phase chromatography.

To confirm the identity of IbTX-D19Y/Y36F, its amino acid sequence was determined after reduction and carboxymethylation (of an uncyclized, but reversed-phase HPLC-purified toxin preparation) by automated Edman degradation (Figure 1D); 35 out of 37 residues were well resolved. However, the two arginine residues at positions 25 and 34 were not detected. Thus, IbTX-D19Y/Y36F was subjected to proteolysis by endoproteinase Lys-C, and the isolated fragments were re-purified by reversed-phase HPLC. Three out of the four isolated peptide fragments (labeled A, B, and C in Figure 1D) yielded amino acid sequence upon automated Edman degradation whereas the fourth fragment did not. This fragment was subjected to electrospray mass spectroscopy. The molecular mass obtained from this fragment revealed

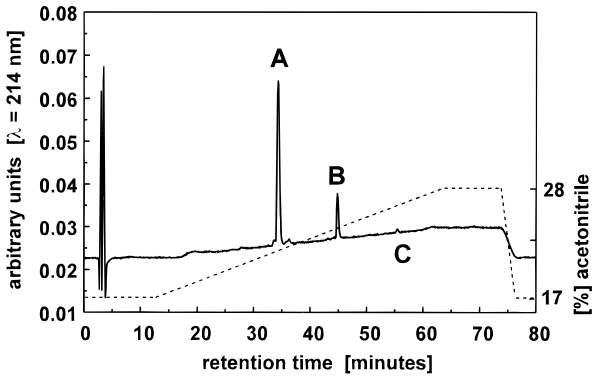

FIGURE 2: Iodination of IbTX-D19Y/Y36F and HPLC separation of iodinated derivatives. IbTX-D19Y/Y36F was subjected to iodination using the Enzymobead method as described under Experimental Procedures. The reaction mixture was loaded onto a HPLC C_{18} reversed-phase column (Vydac C_{18} 0.45 × 25 cm) equilibrated with 17% acetonitrile, 0.05% TFA, and elution was achieved with a linear gradient (17−28%) of acetonitrile in 0.05% TFA applied over 45 min at a flow rate of 1 mL/min. Material eluting from the column was monitored by measuring absorbance at 214 nm/280 nm and, in the case of reaction with [^{125}I]Na, on-line detection of radioactivity. Peaks A, B, and C correspond to unmodified IbTX-D19Y/Y36F, mono-iodo-tyrosine-IbTX-D19Y/Y36F, and di-iodo-tyrosine-IbTX-D19Y/Y36F, respectively.

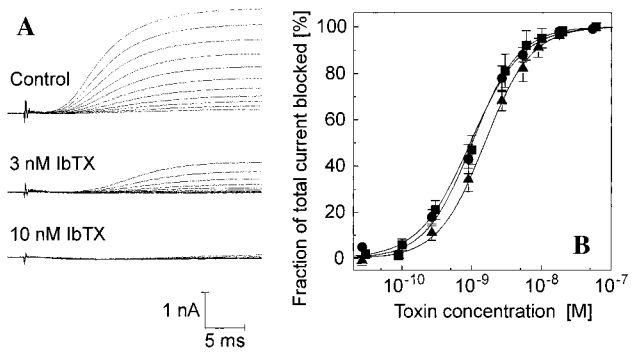

FIGURE 3: Inhibition of maxi-K channels by synthetic IbTX, IbTX-D19Y/Y36F, and the mono-iodo-tyrosine adduct, [^{127}I]IbTX-D19Y/Y36F. Maxi-K channels (hbr1 variant) were expressed in *Xenopus* oocytes and assayed using a two-electrode voltage clamp in the absence or presence of increasing concentrations of IbTX. (A) The membrane potential was clamped at −80 mV and stepped to between 0 mV and +100 mV in 10 mV increments. Top traces, current responses in an oocyte 48 h after injecting hbr1 RNA; middle traces, current responses after 20 min of perfusion with 3 nM IbTX-D19Y/Y36F; bottom traces, current responses after 10 min of perfusion with 10 nM IbTX-D19Y/Y36F. (B) Dose−response curves for synthetic IbTX (●; K_i = 0.94 nM), IbTX-D19Y/Y36F (■; K_i = 1.01 nM), and [^{127}I]IbTX-D19Y/Y36F (▲; K_i = 1.52 nM). The fraction of the total current blocked by toxin at +100 mV is plotted as a function of the toxin concentration. Each data point represents the mean ± SEM of between four and eight independent experiments.

unequivocally that it corresponded to residues 1−11 which spontaneously cyclized during the subsequent experimental manipulations (data not shown). Amino acid sequence obtained from fragments B and C indicated the presence of an arginine residue at positions 25 and 34. Thereafter, all sequencing data were confirmed by electrospray mass spectroscopy (Figure 1E). The mass spectral analysis confirmed that only one component was present in the purified preparation, which possessed a molecular weight of 4278 Da. This number is nearly identical to the calculated molecular weight of folded IbTX-D19Y/Y36F (4277.85 Da). Repeating the mass spectral analysis after cyclizing the amino terminal glutamic acid residue again yielded only one major component, but the molecular weight was lowered to 4263 Da, indicating complete cyclization. Complete cyclization was further assessed by automated Edman degradation. In the first sequencing cycles, no amino acid residues were detected, although 500 pmol of IbTX-D19Y/Y36F had been subjected to analysis (data not shown).

Oxidative Iodination of IbTX-D19Y/Y36F. In order to obtain a high specific activity ligand with marked specificity for maxi-K channels, IbTX-D19Y/Y36F was reacted with [^{125}I]Na as described under Experimental Procedures, and the resulting products were separated by C_{18} reversed-phase chromatography (Figure 2). One reaction product was identified as the mono-iodo adduct of IbTX-D19Y/Y36F on the basis of specific activity corresponding to the maximum theoretical value for incorporation of one iodine per peptide molecule, on mass spectroscopy and on retention time (see below). Under our chromatography conditions, [^{125}I]IbTX-D19Y/Y36F elutes as a well-separated peak, ∼10 min after the underivatized IbTX-D19Y/Y36F (see Figure 2). To confirm that Tyr19 is the iodine-modified residue, uncyclyzed IbTX-D19Y/Y36F was iodinated under identical conditions with [^{127}I]Na and subjected to automated Edman degradation. As expected, automated Edman degradation did not detect a Tyr residue in sequencing cycle 19 but did reveal a distinct peak with higher retention time, suggesting its covalent modification by iodine. Additionally, this toxin sample was subjected to mass spectral analysis which yielded a molecular weight of 4389.0 Da, as expected for mono-iodo-IbTX-D19Y/Y36F (data not shown). Although this mono-iodo adduct is preferentially observed under our experimental conditions, a second iodinated species (6−11% of the total incorporated radioactivity) was detected in each of the individual iodinations. The fact that this iodinated IbTX-D19Y/Y36F derivative represents a di-iodinated toxin species was verified by mass spectral analysis, which indicated a molecular weight of 4515.2 Da. Di-iodo-[^{125}I]IbTX-D19Y/Y36F displays full biological activity as revealed in radioligand binding studies, but it was not further characterized in detail (data not shown).

Functional Characterization of IbTX, IbTX-D19Y/Y36F, and [^{127}I]IbTX-D19Y/Y36F. In order to test whether IbTX-D19Y/Y36F and its mono-iodo derivative retain biological activity, the maxi-K channel α-subunit (hbr1; Tseng-Crank et al., 1994) was expressed in *X. laevis* oocytes and channel function was monitored using a two-electrode voltage clamp (Figure 3). Expression levels under these conditions ranged from 2 to 5 nA of current at 100 mV (Figure 3A). Uninjected or mock-injected oocytes expressed less than 0.15 nA of current (data not shown). The slow activation kinetics under these conditions are due to low levels of endogenous Ca^{2+} (DiChiara & Reinhart, 1995) and a delay to reach voltage clamp conditions due to the large capacitance of oocytes. Steady-state currents were always observed by 30 ms after the voltage step (Figure 3A); hence, all current values were recorded at 30 ms. The toxin washin kinetics were concentration dependent and ranged from 1−2 min for the highest toxin concentrations to 20−30 min for 0.1−0.3 nM IbTX. Dissociation kinetics were not accurately determined since more than 60 min of washout (data not shown) were required to reach equilibrium. The effects of 3 nM and 10 nM IbTX-D19Y/Y36F on oocyte currents are shown in Figure 3A.

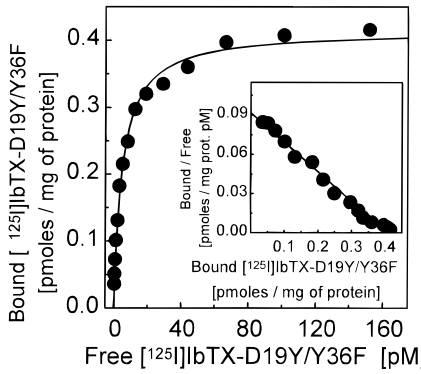

FIGURE 4: Binding properties of [^{125}I]IbTX-D19Y/Y36F to bovine tracheal smooth muscle sarcolemmal membrane vesicles. (A) Saturation binding analysis. Sarcolemmal membranes (3.3 μg/mL) were incubated with increasing concentrations (0.53−153.5 pM) of [^{125}I]IbTX-D19Y/Y36F. The incubation medium consisted of 20 mM Tris/HCl, pH 7.4, 10 mM NaCl, and 0.1% BSA. The binding reaction was carried out at 22 °C until equilibrium was achieved. Specific binding (●, solid line) was assessed from the difference between total and nonspecific binding. For this experiment, a K_d of 5.2 pM and a B_{max} of 0.42 pmol/mg of protein was measured. Inset, specific binding data presented in the form of a Scatchard representation.

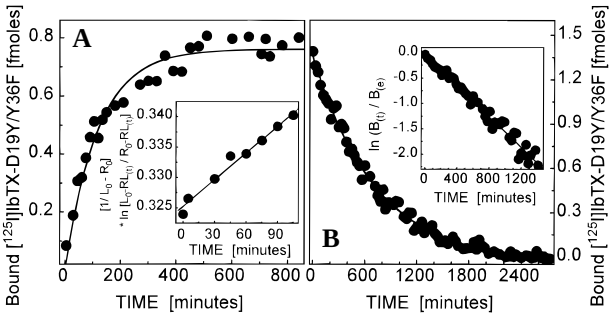

FIGURE 5: Kinetics of [^{125}I]IbTX-D19Y/Y36F to bovine tracheal smooth muscle sarcolemmal membrane vesicles. (A) Association kinetics. 2.06 pM receptor was incubated at 22 °C with 4.41 pM [^{125}I]IbTX-D19Y/Y36F for the indicated periods of time. Nonspecific binding was determined in the presence of 10 nM ChTX. In this experiment an association reaction is depicted. An equilibrium binding level of 0.84 fmol corresponding to 0.076 pmol/mg of protein was measured. (B) Dissociation kinetics. After 3.57 pM tracheal smooth muscle maxi-K channels was incubated with 4.89 pM [^{125}I]IbTX-D19Y/Y36F for 24 h at 22 °C, toxin dissociation was initiated by addition of 10 nM ChTX for the indicated periods of time. An equilibrium binding level of 1.46 fmol corresponding to 0.139 pmol/mg of protein was measured. In this experiment dissociation of 2.3×10^{-5} s^{-1} was determined. Inset, a semilogarithmic representation of the first-order dissociation reaction.

Dose−response data for recombinant wild-type IbTX, IbTX-D19Y/Y36F, and mono-iodo-IbTX-D19Y/Y36F are shown in Figure 3B. For recombinant IbTX, we observed a half-maximal block of channel activity at a concentration of 0.94 nM. Complete abolition of channel activity was seen at 20 nM IbTX (Figure 3B). These data are in excellent agreement with results previously reported for native IbTX block of maxi-K channel activity in excised outside-out patches from primary bovine aortic smooth muscle cells (Galvez et al., 1990) or after channel incorporation into planar lipid bilayers (Giangiacomo et al., 1992). Quantitatively similar data were obtained when either IbTX-D19Y/Y36F or its mono-iodo-tyrosine adduct, [^{127}I]IbTX-D19Y/Y36F, were investigated under these experimental conditions. The affinities of unlabeled and iodine-labeled IbTX analogues were nearly identical (K_i of 1.01 and 1.52 nM, respectively), and both analogues exhibited a kinetic profile similar to that of wild-type IbTX (data not shown). Thus, these data indicate that IbTX-D19Y/Y36F, as well as the mono-iodinated toxin congener block maxi-K channels with an affinity and kinetic profile very similar to that of wild-type IbTX.

Binding Properties of [^{125}I]IbTX-D19Y/Y36F in Purified Bovine Tracheal Smooth Muscle Sarcolemmal Membrane Vesicles. To determine whether [^{125}I]IbTX-D19Y/Y36F can be used to characterize the biochemical and pharmacological properties of maxi-K channels, the binding properties of the mono-iodinated toxin analogue to receptor sites in purified bovine tracheal smooth muscle sarcolemmal membrane vesicles were studied. This tissue was chosen because of the prevalence of maxi-K channels, as well as the fact that their molecular properties (i.e., primary sequences subunit composition and pharmacology) have previously been unequivocally established (Williams et al., 1988; Garcia-Calvo et al., 1994; Knaus et al., 1994b). When membrane vesicles were incubated with increasing concentrations of [^{125}I]IbTX-D19Y/Y36F until equilibrium was achieved, the toxin associated with these membranes in a concentration-dependent manner (Figure 4). In the presence of 10 nM ChTX or IbTX (to determine nonspecific binding), toxin association with membranes was found to be a linear function of the [^{125}I]IbTX-D19Y/Y36F concentration. Specific binding defined as the difference between total binding and binding in the presence of excess competing peptide, was a saturable function of the [^{125}I]IbTX-D19Y/Y36F concentration. A Scatchard analysis of these data (Figure 4, inset) indicated the presence of a single class of binding sites with a K_d of 4.4 pM and a B_{max} of 0.45 pmol/mg of protein. Identical binding parameters have been measured for purified bovine aortic smooth muscle sarcolemmal membrane vesicles (data not shown). Under similar conditions, [^{125}I]ChTX labeled bovine tracheal smooth muscle maxi-K channels with lower affinity ($K_d \approx 20$ pM) whereas the respective B_{max} value was very similar (Vázquez et al., 1989).

The kinetics of [^{125}I]IbTX-D19Y/Y36F binding have been measured to determine whether toxin association occurs through a simple bimolecular reaction. The data presented in Figure 5A indicated that incubation of [^{125}I]IbTX-D19Y/Y36F with a smooth muscle sarcolemmal membrane preparation, under non saturating conditions, resulted in time-dependent association of toxin which approaches equilibrium after ∼12 h. The nonspecific binding component, as determined in the presence of excess ChTX, was time-independent and was subtracted from the experimental determination. Subjecting these data to a transformation according to the second-order rate equation yielded a linear dependence, and the slope of this line gives k_{+1} (Figure 5A, inset). The mean association rate constant, k_{+1}, calculated from three independent experiments was determined to be 2.4×10^6 M^{-1} s^{-1}. This value is close to the diffusion control rate expected for a small peptide, and suggests that no significant long-range electrostatic interactions occur between toxin and negative charges at the channel's outer vestibule. Supporting this finding, a similar number (1.3×10^6 M^{-1} s^{-1}) was determined when the IbTX association kinetics were examined for smooth muscle maxi-K channels by measuring single-channel events after incorporation of channels into planar lipid bilayers (Giangiacomo et al., 1992).

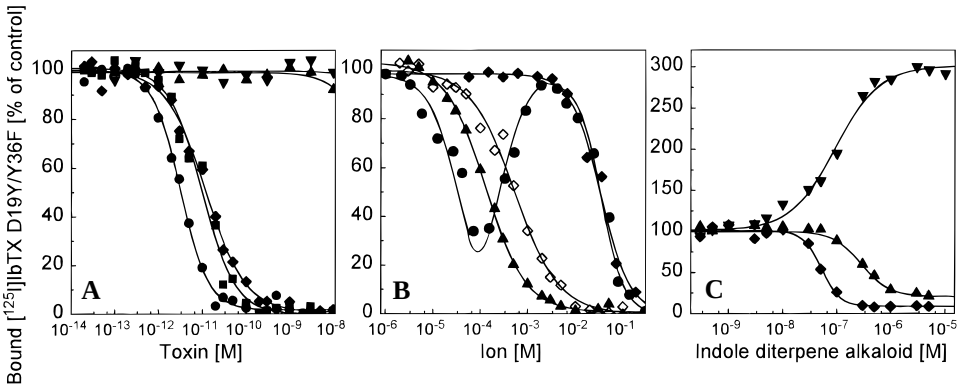

FIGURE 6: Pharmacological profile of [^{125}I]IbTX-D19Y/Y36F binding to bovine tracheal smooth muscle sarcolemmal membrane vesicles. For all experiments shown in this figure, tracheal membrane vesicles (3.1−4.6 μg/mL) were incubated with 2.0−4.1 pM [^{125}I]IbTX-D19Y/Y36F in the absence or presence of increasing concentrations of modulators. (A) Synthetic IbTX (■, IC_{50} 27.4 pM, n_H 1.02), IbTX-D19Y/Y36F (◆, IC_{50} 31.6 pM, n_H 0.99), ChTX (●, IC_{50} 4.2 pM, n_H 1.61), MgTX (▼), or α-DaTX (▲) at 22 °C for 12 h. Inhibition of these toxins was assessed relative to an untreated control. (B) $CaCl_2$, KCl, NaCl, and TEA. The experimental conditions are as described in A. $CaCl_2$ (◇, IC_{50} 0.61 mM, n_H 0.98), KCl (●) IC_{50} (I) 21 μM; EC_{50} (II) 284 μM; IC_{50} (III) 23.4 mM, NaCl (◆, IC_{50} 28 mM, n_H 1.01) and TEA (▲, IC_{50} 0.12 mM, n_H 1.01). (C) Increasing concentrations of verruculogen (▼, EC_{50} 92.1 nM, n_H 1.06), aflatrem (▲, IC_{50} 284 nM, n_H 1.71), or penitrem A (◆, IC_{50} 52.4 nM, n_H 2.52) were incubated with [^{125}I]IbTX-D19Y/Y36F and bovine tracheal smooth muscle membranes. Under control conditions 3−5% of receptor sites are occupied by [^{125}I]IbTX-D19Y/Y36F. All displacement curves were computer-fitted to the general dose−response curve as described in Experimental Procedures.

Dissociation of [^{125}I]IbTX-D19Y/Y36F from its receptor, initiated by addition of excess ChTX, displayed a single mono-exponential relationship with a $t_{1/2}$ of ∼8 h (k_{-1} of 1.8×10^5 s^{-1}; Figure 5B). The K_d calculated from these kinetic constants is 7.5 pM, a value very similar to the one determined under equilibrium binding conditions (4.4 pM). When the temperature dependence of the binding reaction was investigated at 22 or 37 °C (binding experiments at 4 °C were not performed due to the slow association rate of IbTX), binding at 37 °C was found to represent ∼50% of the level measured at 22 °C (data not shown). In summary, given the very low degree of nonspecific binding, its high affinity, slow dissociation as well as its selectivity for maxi-K channels (see below), [^{125}I]IbTX-D19Y/Y36F exhibits definite advantages over [^{125}I]ChTX for the study of maxi-K channels.

Pharmacological Properties of [^{125}I]IbTX-D19Y/Y36F Binding to Bovine Tracheal Smooth Muscle Sarcolemmal Membranes. To ascertain whether wild-type IbTX or noniodinated IbTX-D19Y/Y36F display a similar affinity for the receptor as [^{125}I]IbTX-D19Y/Y36F, competition experiments were performed. The corresponding data are shown in Figure 6A and have been subjected to data analysis according to (Linden, 1982). Wild-type IbTX, as well as IbTX-D19Y/Y36F, displaced [^{125}I]IbTX-D19Y/Y36F binding from maxi-K channels with a K_i value of 7 pM in the presence of 10 mM NaCl, a number equivalent to the K_d measured in direct saturation experiments with the iodinated ligand (see Figure 4). Therefore, these data together with the functional data presented above demonstrate that substitution of two residues within the primary amino acid structure of IbTX and iodination of one of these residues do not cause any significant loss in toxin affinity.

To investigate the pharmacological characteristics of smooth muscle maxi-K channels labeled with [^{125}I]IbTX-D19Y/Y36F, structurally related (ChTX, MgTX) and unrelated (α-DaTX) K^+ channel toxins were tested for their ability to modulate the binding reaction (Figure 6A). Of all these toxins, only ChTX was capable of inhibiting binding of [^{125}I]IbTX-D19Y/Y36F in a dose-dependent manner (K_i ≈ 4 pM). In contrast, toxins with a defined selectivity for certain types of voltage-gated K^+ channels (e.g., MgTX or α-DaTX) showed no significant inhibition of [^{125}I]IbTX-D19Y/Y36F binding up to concentrations of 10 nM (Figure 6A).

Several ions such as K^+, TEA, and Ca^{2+} which are known to interact with smooth muscle maxi-K channels by binding to sites along the ion conduction pathway, and which have been shown to modulate [^{125}I]ChTX binding to maxi-K channels (Vázquez et al., 1989; McManus et al., 1995) were also investigated. When membrane vesicles were incubated with [^{125}I]IbTX-D19Y/Y36F and increasing concentrations of either Ca^{2+} or TEA, a concentration-dependent inhibition of toxin binding is observed (Figure 6B). K_i values for Ca^{2+} and TEA are 610 and 132 μM, respectively. For TEA, this value was equivalent to its reported affinity not only as an inhibitor of maxi-K channels (Miller, 1988), but also for displacing [^{125}I]ChTX binding to smooth muscle membranes (Vázquez et al., 1989). For K^+, we observed a complex interaction profile with [^{125}I]IbTX-D19Y/Y36F binding (Figure 6B). At low potassium concentrations, this monovalent cation partially inhibited binding of [^{125}I]IbTX-D19Y/Y36F, with an IC_{50} value close to the one reported for K^+ inhibition of [^{125}I]ChTX binding to smooth muscle membranes (30 μM) (Vázquez et al., 1989). As K^+ was further increased in the low mM range, partial reversal of the inhibition of [^{125}I]IbTX-D19Y/Y36F binding was observed. This is a phenomena which had previously been described for [^{125}I]ChTX and [^{125}I]MgTX binding to voltage-gated K^+ channels in rat brain synaptic membranes (Vázquez et al., 1990; Knaus et al., 1995). Further increase in K^+ concentration was followed by a complete inhibition of [^{125}I]IbTX-D19Y/Y36F binding to smooth muscle membranes. This pattern is observed only in the presence of K^+, but not with other monovalent cations such as Na^+ or Li^+, indicating a specificity to the K^+ interaction.

Indole diterpene alkaloids have been shown to bind specifically to smooth muscle maxi-K channels and to modulate [^{125}I]ChTX binding to this channel in either a positive or negative allosteric manner (Knaus et al., 1994c). Therefore, we investigated the effects of this class of compounds on [^{125}I]IbTX-D19Y/Y36F binding to maxi-K

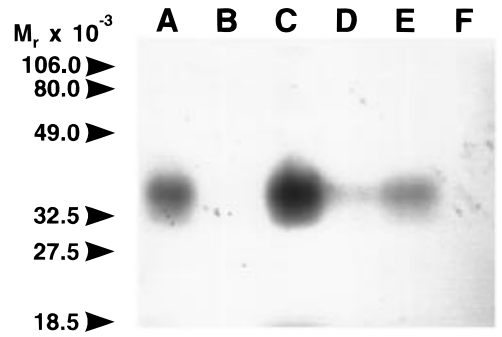

FIGURE 7: Effects of various modulators on covalent incorporation of [^{125}I]IbTX-D19Y/Y36F into the β-subunit of high-conductance Ca^{2+}-activated K^+ channels. Bovine tracheal smooth muscle sarcolemmal membrane vesicles (~40 μg) were incubated with 35.5 pM [^{125}I]IbTX-D19Y/Y36F under control conditions (A) or the presence of 10 nM ChTX (B), 3 μM paxilline (C), 3 μM aflatrem (D), 1 mM KCl (E), or 1 mM TEA (F) at 2 °C until equilibrium was achieved. Samples were subjected to the cross-linking reaction employing DSS and separated by SDS−PAGE as described under Experimental Procedures. The migration of molecular weight standards is shown.

channels. As reported for [^{125}I]ChTX, [^{125}I]IbTX-D19Y/Y36F binding is stimulated by verruculogen (Figure 6C). However, negative allosteric regulators, such as aflatrem or penitrem A, were inhibitory with K_i values very close to the ones reported for [^{125}I]ChTX binding to smooth muscle membranes (Figure 6C).

An alternative approach to demonstrate a specific interaction of [^{125}I]IbTX-D19Y/Y36F with smooth muscle maxi-K channels is to monitor its pattern of covalent incorporation into the maxi-K channel β-subunit. It has previously been shown using the protocol outlined in Experimental Procedures that [^{125}I]ChTX can be specifically incorporated into the β-subunit and its incorporation is modulated by agents that either inhibit or stimulate the reversible binding reaction (Knaus et al., 1994c). In a similar fashion, maxi-K channels were labeled with [^{125}I]IbTX-D19Y/Y36F in the absence or presence of competing toxins or indole diterpene alkaloids. The bifunctional cross-linking reagent, disuccinimidyl suberate, was used to achieve covalent incorporation of toxin into its receptor. [^{125}I]IbTX-D19Y/Y36F specifically labeled the β-subunit of the maxi-K channel (Figure 7); all agents which inhibit reversible binding prevented incorporation, while stimulators of the binding reaction increased the level of toxin incorporation. Thus, the pharmacology characteristic of reversible [^{125}I]IbTX-D19Y/Y36F binding is mirrored in the pattern of the toxin's irreversible incorporation into the β-subunit, a finding which provides additional proof for a specific [^{125}I]IbTX-D19Y/Y36F interaction.

[^{125}I]IbTX-D19Y/Y36F Is a Selective Ligand for Maxi-K Channels. In order to extend the pharmacology of [^{125}I]-IbTX-D19Y/Y36F and to obtain additional evidence for specificity, we investigated the binding profile of this ligand with rat brain synaptic plasma membrane vesicles (Table 1). In this tissue, the dissociation constant, as well as the maximal density of sites labeled by [^{125}I]IbTX-D19Y/Y36F, was very similar to those values found in smooth muscle membranes. [^{125}I]IbTX-D19Y/Y36F bound to a single class of sites with a K_d of ~20 pM and a site density of 0.4 pmol/mg of protein. Wild-type IbTX, IbTX-D19Y/Y36F, and ChTX completely inhibited [^{125}I]IbTX-D19Y/Y36F binding to this membrane preparation (Table 1). Neither MgTX nor α-DaTX showed any inhibition, up to concentrations of 10 nM. Moreover, no specific binding of [^{125}I]IbTX-D19Y/Y36F was observed to membranes derived from HEK-293 or CHO cells, which have been stably transfected with a number of different voltage-gated K^+ channels (K_v1.1, K_v1.2, or K_v1.3; data not shown). However, these plasma membranes expressed high levels of binding for either [^{125}I]α-DaTX or [^{125}I]MgTX. Finally, IbTX-D19Y/Y36F did not inhibit binding of [^{125}I]MgTX, [^{125}I]α-DaTX, and even more importantly, [^{125}I]ChTX to rat brain synaptosomal membrane vesicles. For these radioligands it has been shown that the voltage-gated K^+ channel K_v1.2 (and perhaps K_v1.1 as well as K_v1.3) constitute their high-affinity receptor in mammalian brain (Scott et al., 1990; Grissmer et al., 1994; Chandy & Gutman, 1995). In summary, introducing two amino acid substitutions into IbTX at positions 19 and 36 does not result in any detectable alteration of its pharmacological profile of this ligand but provides a tool with which to obtain a selective, high specific activity radioligand for maxi-K channels.

Table 1: Binding Profile of [^{125}I]IbTX-D19Y/Y36F to Rat Brain Synaptosomal Plasma Membrane Vesicles

displacer (K_i; [pM])	[^{125}I]IbTX D19Y/Y36F	[^{125}I]ChTX	[^{125}I]MgTX	[^{125}I]α-DaTX
IbTX	21.1	>10 000	>10 000	>10 000
IbTX-D19Y/Y36F	22.5	>10 000	>10 000	>10 000
ChTX	17.0	4.0	5.1[a]	59.0
MgTX	>10 000	10.9	0.15[a]	0.6
α-DaTX	>10 000	11.3	0.49[a]	0.4
β-DaTX	>10 000	80.9	2.1	3.1
γ-DaTX	>10 000	1300.0	20.3	29.7
δ-DaTX	>10 000	225.0	6.6	2.8

[a] K_i values taken from Knaus et al. (1995).

DISCUSSION

Until now, [^{125}I]ChTX was the only available high specific activity ligand to probe maxi-K channels and served a very important role in the purification of maxi-K channels from airway and aortic smooth muscle (Vázquez et al., 1989; Garcia-Calvo et al., 1994). However, the pharmacological characterization of maxi-K channels in most other tissues of interest was difficult since [^{125}I]ChTX also binds with high affinity to members of the *Shaker* voltage-gated K^+ channels (e.g., K_v1.2 and K_v1.3) that are expressed in the mammalian CNS or in endocrine tissues (Wang et al., 1994; Chandy et al., 1993). Similarly, ChTX binds to other types of Ca^{2+}-activated K^+ channels; including the intermediate-conductance *Gardos* channel present in the plasma membrane of human red blood cells (Brugnara et al., 1993a,b), and two types of synaptosomal intermediate-conductance channels (Reinhart et al., 1989).

To overcome this inherent problem of [^{125}I]ChTX, we previously attempted to radio-iodinate wild-type IbTX at Tyr36. In striking contrast to ChTX, all attempts to achieve iodination at this position destroy the toxin's biological activity (M.L.G., unpublished results). Recently we developed a strategy to radiolabel an IbTX analogue with [^{3}H] [[^{3}H]NEM-IbTX-C19 (Knaus et al., 1996)]. But due to its low specific activity, this ligand displayed clear disadvantages when compared to an iodinated radioligand. For instance, a high density of receptors is required to achieve a significant binding signal at equilibrium. Based on this limitation, a

different approach was sought to produce radioiodinated IbTX. Studies in which ChTX was subjected to an extensive site-directed mutagenesis paradigm, coupled with the functional screening of these mutant toxins (Stampe et al., 1994), and the fact that the three-dimensional structure of IbTX in solution is very similar to that of ChTX (Bontems et al., 1991, 1992), assisted the construction of an appropriate IbTX analogue. The mutagenesis experiments with ChTX assigned eight residues which are crucial for high-affinity interaction of that toxin with maxi-K channels. Seven out of the eight mapped residues are identical in IbTX, and they have been shown to be located on one face of the toxin molecule. Other residues, among them Asp19, have been shown not to contribute to the interaction surface of the toxin. These ChTX mutagenesis experiments also revealed that Tyr36 is one out of two hydrophobic residues that is essential for high-affinity binding of peptide to maxi-K channels; this might have prevented the successful iodination of biologically active IbTX since this toxin has a Tyr residue in the same position. Replacing this Tyr residue with Phe appears to be permissive (Stampe et al., 1994). Most importantly, the corresponding ChTX double mutant (ChTX-R19Y/Y36F) has been shown to be indistinguishable in terms of its kinetic profile and affinity when compared to wild-type ChTX (Stampe et al., 1994). We have, therefore, chosen to mutate IbTX at positions 19 and 36 to generate a toxin analogue that could be radio-iodinated to high specific activity without impairing its biological activity.

In order to obtain significant amounts of this IbTX analogue, we expressed this peptide as part of a fusion protein in *E. coli*, and subsequently purified it to homogeneity by ion exchange and reversed-phase chromatography. Functional screening of IbTX-D19Y/Y36F and its mono-iodotyrosine adduct, [^{127}I]IbTX-D19Y/Y36F, in electrophysiological experiments indicated an unaltered biological profile with respect to interaction with maxi-K channels: wild-type IbTX, IbTX-D19Y/Y36F, and the mono-iodo-tyrosine adduct, [^{127}I]IbTX-D19Y/Y36F, block maxi-K channels expressed in *Xenopus* oocytes, in a manner which is indistinguishable, both qualitatively and quantitatively from each other. The corresponding K_i values ($\sim$1 nM) for half-maximal channel block are in excellent agreement with results previously obtained for wild-type IbTX using either excised outside-out patches from primary aortic smooth muscle cells (Galvez et al., 1990) or channels incorporated into planar lipid bilayers (Giangiacomo et al., 1992). Additionally, the blocking and unblocking kinetics of IbTX-D19Y/Y36F and [^{127}I]IbTX-D19Y/Y36F did not display any significant difference when compared with wild-type IbTX. All peptides show slow association and dissociation kinetics consistent with previously published electrophysiological data (Giangiacomo et al., 1992).

Additional support for the specificity of [^{125}I]IbTX-D19Y/Y36F as a probe for maxi-K channels was obtained in experiments where the pharmacological profile of the binding reaction in bovine tracheal smooth muscle membranes was characterized. Binding of the radiolabeled toxin analogue is only modulated by compounds which are established blockers of maxi-K channels (ChTX, IbTX, indole diterpene alkaloids, and TEA). The measured K_i values are close, or even identical to what has previously been reported for modulation of [^{125}I]ChTX binding to bovine aortic smooth muscle sarcolemmal membranes (Vázquez et al., 1989). In contrast, selective blockers of voltage-gated K^+ channels (MgTX, α-DaTX) do not exhibit any significant interaction with maxi-K channels that are labeled with [^{125}I]IbTX-D19Y/Y36F. In accordance with these data, IbTX-D19Y/Y36F does not interfere with [^{125}I]MgTX or [^{125}I]α-DaTX binding to brain membranes. In order to obtain an independent set of measurements indicating high specificity of [^{125}I]IbTX-D19Y/Y36F for maxi-K channels, toxin incorporation into the β-subunit was monitored in cross-linking studies. In these experiments, this IbTX analogue was covalently incorporated exclusively into the smooth muscle β-subunit, and modulators of this event absolutely reflect the pharmacological profile of the binding reaction.

In summary, in this paper we introduce for the first time a biologically active IbTX analogue, which can be radiolabeled with ^{125}I at Tyr19. [^{125}I]IbTX-D19Y/Y36F specifically binds to maxi-K channels in both smooth muscle and brain, and the pharmacological profile characterizing the binding reaction clearly indicates an exclusive interaction of this toxin analogue with maxi-K channels. In smooth muscle, this radioligand displays a higher affinity when compared to [^{125}I]ChTX, a finding which could be due to the fact that [^{125}I]ChTX suffers a drop in affinity upon iodination, whereas [^{125}I]IbTX-D19Y/Y36F does not. Moreover, [^{125}I]IbTX-D19Y/Y36F exhibits a better signal-to-noise ratio and a superior kinetic profile than [^{125}I]ChTX, and it appears absolutely selective for maxi-K channels. Taken together, the use of [^{125}I]IbTX-D19Y/Y36F in reversible and irreversible radioligand binding studies will now facilitate a detailed analysis of the channel's pharmacological profile in tissues with low channel abundance, particularly when these tissues simultaneously express a high density of voltage-gated K^+ channels (e.g., brain and neuroendocrine tissues). Likewise, this ligand is expected to serve an important role in determining maxi-K channel distribution (particularly in the CNS) by means of receptor autoradiography, to investigate the channel's subunit composition in target tissues of interest and to facilitate the biochemical purification of maxi-K channel complexes from tissues other than smooth muscle. Given the extremely slow dissociation kinetics of [^{125}I]IbTX-D19Y/Y36F, this ligand appears particularly suited for this latter application.

ACKNOWLEDGMENT

We thank Dr. Reid Leonard for advice in constructing the IbTX-D19Y/Y36F expression plasmid, Dr. Siegmund Wanner and Maria Trieb for technical contributions, and Emanuel Emberger for the toxin expression. Tracy Klatt and Dr. Pat Griffin are gratefully acknowledged for the mass spectroscopy data as is Dr. Hartmut Glossmann for continuous support and discussion. This work is part of the graduate diploma of A.K.

REFERENCES

Anderson, C. S., MacKinnon, R., Smith, C., & Miller, C. (1988) *J. Gen. Physiol. 91*, 317−333.

Arkett, S. A., Dixon, J., Yang, J. N., Sakai, D. D., Minkin, C., & Sims, S. M. (1994) *Receptors Channels. 2*, 281−293.

Bontems, F., Roumestand, C., Boyot, P., Gilquin, B., Doljansky, Y., Menez, A., & Toma, F. (1991) *Eur. J. Biochem. 196*, 19−28.

Bontems, F., Gilquin, B., Roumestand, C., Menez, A., & Toma, F. (1992) *Biochemistry 31*, 7756−7764.

Bradford, M. M. (1976) *Anal. Biochem. 72*, 248−254.

Brugnara, C., De Franceschi, L., & Alper, S. L. (1993a) *J. Clin. Invest. 92*, 520−526.
Brugnara, C., De Franceschi, L., & Alper, S. L. (1993b) *J. Biol. Chem. 268*, 87608768.
Butler, A., Tsunoda, S., McCobb, D. P., Wei, A., & Salkoff, L. (1993) *Science 261*, 221−224.
Chandy, K. G., & Gutman, G. A. (1995) in *Handbook of receptors and channels: ligand and voltage-gated ion channels* (North, R. A., Ed.) pp 1−71, CRC Press, Boca Raton, FL.
Chandy, K. G., Gutman, G. A., & Grissmer, S. (1993) *Semin. Neurosci. 5*, 125−134.
DeLean, A., Munson, P. J., & Rodbard, D. (1978) *Am. J. Physiol. 4*, E97−E102.
Deutsch, C., Price, M., Lee, S., King, V. F., & Garcia, M. L. (1991) *J. Biol. Chem. 266*, 3668−3674.
DiChiara, T. J., & Reinhart, P. H. (1995) *J. Physiol. 439*, 403−418.
Dumont, J. N. (1972) *J. Morphol. 136*, 153−179.
Galvez, A., Gimenez-Gallego, G., Reuben, J. P., Roy-Contancin, L., Feigenbaum, P., Kaczorowski, G. J., & Garcia, M. L. (1990) *J. Biol. Chem. 265*, 11083−11090.
Garcia-Calvo, M., Leonard, R. J., Novick, J., Stevens, S. P., Schmalhofer, W. A., Kaczorowski, G. J., & Garcia, M. L. (1993) *J. Biol. Chem. 268*, 18866−18874.
Garcia-Calvo, M., Knaus, H. G., McManus, O. B., Giangiacomo, K. M., Kaczorowski, G.J., & Garcia, M. L. (1994) *J. Biol. Chem. 269*, 676−682.
Giangiacomo, K. M., Garcia, M. L., & McManus, O. B. (1992) *Biochemistry 31*, 6719−6727.
Giangiacomo, K. M., Garcia-Calvo, M., Knaus, H. G., Mullmann, T. J., Garcia, M. L., & McManus, O. B. (1995) *Biochemistry 34*, 15849−15862.
Gimenez-Gallego, G., Navia, M. A., Reuben, J. P., Katz, G. M., Kaczorowski, G. J., & Garcia, M. L. (1988) *Proc. Natl. Acad. Sci. U.S.A. 85*, 3329−3333.
Grissmer, S., Nguyen, A. N., Aiyar, J., Hanson, D. C., Mather, R. J., Gutman, G. A., Karmilowicz, M. J., Auperin, D. D., & Chandy, K. G. (1994) *Mol. Pharmacol. 45*, 1227−1234.
Hermann, A., & Erxleben, C. (1987) *J. Gen. Physiol. 90*, 27−47.
Kaczorowski, G. J., Knaus, H. G., Leonard, R. J., McManus, O. B., & Garcia, M. L. (1996) *J. Bioenerg. Biomembr. 28*, 253−265.
Knaus, H. G., Folander, K., Garcia-Calvo, M., Garcia, M. L., Kaczorowski, G. J., Smith, M., & Swanson, R. (1994a) *J. Biol. Chem. 269*, 17274−17278.
Knaus, H. G., Garcia-Calvo, M., Kaczorowski, G. J., & Garcia, M. L. (1994b) *J. Biol. Chem. 269*, 3921−3924.
Knaus, H. G., McManus, O. B., Lee, S. H., Schmalhofer, W. A., Garcia-Calvo, M., Helms, L. M. H., Sanchez, M., Giangiacomo, K. M., Reuben, J. P., Smith, A. B., III, Kaczorowski, G. J., & Garcia, M. L. (1994c) *Biochemistry 33*, 5819−5828.
Knaus, H. G., Koch, R. O. A., Eberhart, A., Kaczorowski, G. J., Garcia, M. L., & Slaughter, R. S. (1995) *Biochemistry 34*, 13627−13634.
Knaus, H. G., Schwarzer, C., Koch, R. O. A., Eberhart, A., Kaczorowski, G. J., Glossmann, H., Wunder, F., Pongs, O., Garcia, M. L., & Sperk, G. (1996) *J. Neurosci. 16*, 955−963.
Latorre, R., Oberhauser, A., Labarca, P., & Alvarez, O. (1989) *Annu. Rev. Physiol. 51*, 385−399.
Leonard, R. J., Garcia, M. L., Slaughter, R. S., & Reuben, J. P. (1992) *Proc. Natl. Acad. Sci. U.S.A. 89*, 10094−10098.
Linden, J. (1982) *J. Cyclic Nucleotide Res. 8*, 163−172.
MacKinnon, R., & Miller, C. (1988) *J. Gen. Physiol. 91*, 335−349.
McManus, O. B., Harris, G. H., Giangiacomo, K. M., Feigenbaum, P., Reuben, J. P., Addy, M. E., Burka, J. F., Kaczorowski, G. J., & Garcia, M. L. (1993) *Biochemistry 32*, 6128−6133.
McManus, O. B., Pallanck, L., Helms, L. M. H., Swanson, R., & Leonard, R. J. (1995) *Neuron 14*, 645−650.
Miledi, R. (1982) *Proc. R. Soc. London 215*, 492−497.
Miller, C. (1988) *Neuron 1*, 1003−1006.
Miller, C., Moczydlowski, E., Latorre, R., & Philips, M. (1985) *Nature 313*, 316−318.
Oosawa, Y., Ashcroft, S. J., & Ashcroft, F. M. (1992) *Diabetologia 35*, 619−623.
Park, C.-S., Hausdorff, S. F., & Miller, C. (1991) *Proc. Natl. Acad. Sci. U.S.A. 88*, 2046−2050.
Rane, S. G. (1991) *Am. J. Physiol. 260*, C104−C112.
Reinhart, P. H., Chung, S., & Levitan, I. B. (1989) *Neuron 2*, 1031−1041.
Sanger, F., Nicklen, S., & Coulson, A. R. (1977) *Proc. Natl. Acad. Sci. U.S.A. 74*, 5463−5467.
Scott, V. E. S., Parcej, D. N., Keen, J. N., Findlay, J. B., & Dolly, J. O. (1990) *J. Biol. Chem. 265*, 20094−20097.
Slaughter, R. S., Shevell, J. L., Felix, J. P., Garcia, M. L., & Kaczorowski, G. J. (1989) *Biochemistry 28*, 3995−4002.
Solaro, C., & Lingle, C. (1992) *Science 257*, 1694−1698.
Stampe, P., Kolmakova Partensky, L., & Miller, C. (1994) *Biochemistry 33*, 443−450.
Tseng-Crank, J., Foster, C. D., Krause, J. D., Mertz, R., Godinot, N., DiChiara, T. J., & Reinhart, P. H. (1994) *Neuron 13*, 1315−1330.
Van Renterghem, C., & Lazdunski, M. (1992) *Pflügers Arch. 420*, 417−423.
Vázquez, J., Feigenbaum, P., Katz, G., King, V. F., Reuben, J. P., Roy-Contancin, L., Slaughter, R. S., Kaczorowski, G. J., & Garcia, M. L. (1989) *J. Biol. Chem. 264*, 20902−20909.
Vázquez, J., Feigenbaum, P., King, V. F., Kaczorowski, G. J., & Garcia, M. L. (1990) *J. Biol. Chem. 265*, 15564−15571.
Wang, H., Kunkel, D. D., Schwartzkroin, P. A., & Tempel, B. L. (1994) *J. Neurosci. 14*, 4588−4599.
Wang, X., Inukai, T., Greer, M. A., & Greer, S. E. (1994) *Brain. Res. 662*, 83−87.
Williams, J. R., Katz, G. M., Roy-Contancin, L., & Reuben, J. P. (1988) *Proc. Natl. Acad. Sci. U.S.A. 85*, 9360−9364.
Zweifach, A., Desir, G. V., Aronson, P. S., & Giebisch, G. H. (1991) *Am. J. Physiol. 261*, F187−F196.

BI962074M